CONFERENCE PRE-PRINT

QUANTITATIVE EVALUATION OF BEAM LOSS BASED ON RADIATION DETECTION IN HIGH-DUTY BEAM COMMISSIONING OF LIPAC RFQ

K. KUMAGAI, K. HASEGAWA, K. KONDO, S. KWON, K. MASUDA, K. OCHIAI QST-Rokkasho Aomori, Japan Email: kumagai.kohki@qst.go.jp

Y. CARIN, H. DZITKO Fusion for Energy Aomori, Japan

D. JIMENEZ-REY CIEMAT Madrid, Spain

V. LOPEZ UNED Madrid, Spain

Abstract

Using the LIPAc deuteron accelerator, beam loss characteristics were quantitatively assessed using multiple radiation measurement techniques. Elevated dose rates and isotope production at the interface between the MEBT Extension Line (MEL) and the HEBT indicate significant losses of high-energy core particles. In contrast, HPGe spectroscopy and energy-dependent calculations confirmed that halo particles lost at the HEBT magnet had lower deuteron energies than core particles. Activation foil data further validated beam losses of core and halo particles. These findings highlight the effectiveness of multi-radiation diagnostics in characterizing beam loss and enhancing radiation safety in the accelerator environment.

1. INTRODUCTION

The IFMIF/EVEDA project [1] is being conducted under the Broader Approach agreement between the government of Japan and EURATOM. As part of these activities, beam commissioning of the Linear IFMIF Prototype Accelerator (LIPAc) takes place at Rokkasho, Japan, aiming at demonstrating the feasibility of high-intensity deuteron beam acceleration in continuous wave (CW) mode. Fig. 1 shows a top view of the LIPAc in its "Phase-B+" [1] configuration, which features the Medium-energy beam transport Extension Line (MEL) in place of the superconducting RF linac. In this configuration, the Phase-B+ beam achieved a deuteron beam current of approximately 120 mA, with acceleration up to 5 MeV using the radiofrequency quadrupole (RFQ). In high-current ion beam accelerators, controlling beam loss within acceptable limits is a critical challenge, as excessive loss can lead to severe damage and activation of beamline components. To address this issue, a detailed investigation of beam loss mechanisms including contributions from both core and halo particles was performed using multiple radiation diagnostics, providing essential insights for upcoming 9 MeV LIPAc accelerator operations in Phase-C/D.

During the Phase-B+ campaign, unexpected beam losses were detected by twenty-one ionization chambers (ICs) installed along the MEBT, MEL, and HEBT lines [2]. These ICs, shown as thin yellow cylinders in Fig. 1, are photon-sensitive monitors that provided qualitative indications of beam loss, although the photon flux entering the chambers could not be quantitatively measured. Fig. 1 also shows nickel activation foil measurement results, represented by coloured circles placed on the beam duct surface during a net nine-day beam operation from 17 to 27 June 2024. Elevated reaction rates were observed at the positions marked with black, orange, and yellow circles. These measurements revealed multiple localized loss points, with the highest reaction rate observed at the D-Plate graphite slit, where secondary neutrons were generated during beam shape diagnostics via deuteron-graphite interactions during slit insertion. Additional activation was detected at the MEL-HEBT interface, the HEBT magnet (HMA06 exit), and the HEBT scraper. To quantitatively assess beam loss, this study employed a NaI(Tl) survey meter, a portable High-Purity Germanium (HPGe) detector, and activation foils, enabling absolute

evaluation of loss characteristics and contributing to a deeper understanding of loss mechanisms in high-intensity accelerator operation.

Fig. 1 Top view of the LIPAc accelerator in the Phase-B+ configuration. The photo on the right shows the actual ionization chambers used during the Phase-B+ beam operation.

METHODS

Beam operations during Phase-B+ were conducted from July 2021 to June 2024, typically between 10:00 AM and 5:00 PM on weekdays. Fig. 2 shows the signals recorded by the AC Current Transformer (ACCT), installed at the second triplet, and five beam loss monitors (IC-1 to IC-5, as shown in Fig. 1), during beam operations on June 10, 17, and 18, 2024. IC-1 to IC-3 and IC-4 to IC-5 monitored beam losses near the MEL-HEBT interface and the HEBT magnet (HMA06 exit), respectively, where significant losses were detected using a NaI(Tl) survey meter (ALOKA Co., Ltd., model TCS-172). As shown in Fig. 2, pronounced beam losses were observed on June 10, characterized by consistently elevated loss levels throughout the operation. On June 17, sudden beam losses occurred at the MEL-HEBT interface (around 16:25) and at the HEBT magnet (at 16:35 and 17:10). In contrast, no distinct losses were observed on June 18. Nevertheless, as discussed in Section 3, increased dose rates and foil activation were detected on June 18, indicating the presence of beam loss. These results demonstrate that even small losses, which cannot be observed by ICs, can be effectively detected using the NaI(Tl) survey meter and activation foil measurements.

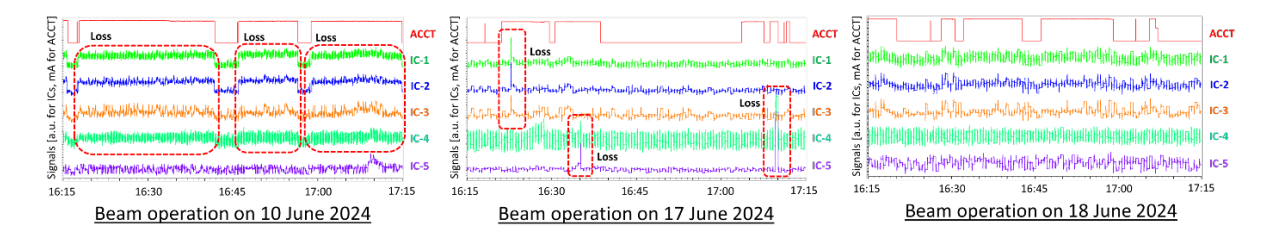


Fig. 2 Representative signal profiles from beam loss monitors (IC-1 to IC-5) recorded during beam operations on June 10, 17, and 18, 2024.

During the Phase-B+ campaign, dose rates were measured using a NaI(Tl) survey meter at multiple locations along the beamline to identify daily beam losses, as shown in Fig. 3. The time constant was typically set to 10 seconds, and measurements at each point were taken for over 30 seconds. Although the method is relatively simple, the portability of the NaI(Tl) survey meter makes it an effective tool for locating beam loss. Approximate loss levels were inferred from daily variations in dose rate. These measurements were compared with simulations performed using a combination of the Monte Carlo code MCNP6 [3] and the activation code FISPACT-II [4]. First, deuteron deceleration in the beam duct was calculated to obtain the flux and the energy spectrum based on the CCFE 162-group structure using MCNP for the MEL-HEBT interface and the HMA06 exit, with the latest prototype JENDL-5 deuteron sublibrary for Fe(d,x) reactions. Second, total gamma yield (per cm³ per second) and energy spectra were calculated using FISPACT-II, assuming a constant beam loss (e.g. 10 µA) during injection. The irradiation time considered actual beam-on durations and duty cycles, typically around 1%. As shown in Fig. 3, simplified geometries were adopted for the MEL-HEBT interface and the HMA06 exit in the MCNP calculations. Due to localized damage at the flange edge of the MEL-HEBT interface, where the pipe diameter narrows like a collimator, a point photon source was defined vertically in the MCNP model. For the MCNP calculations at the HMA06 exit shown in Fig. 3(b), based on the relatively broad high-dose region observed in the NaI(Tl) measurements, a surface photon source was defined in the -X direction. Lost deuterons were assumed to be monoenergetic (e.g. 5 MeV) in the initial MCNP source definition. Finally, the dose rates at the NaI(Tl) scintillator positions for the MEL-HEBT interface and the HMA06 exit were calculated using MCNP with the gamma yields.

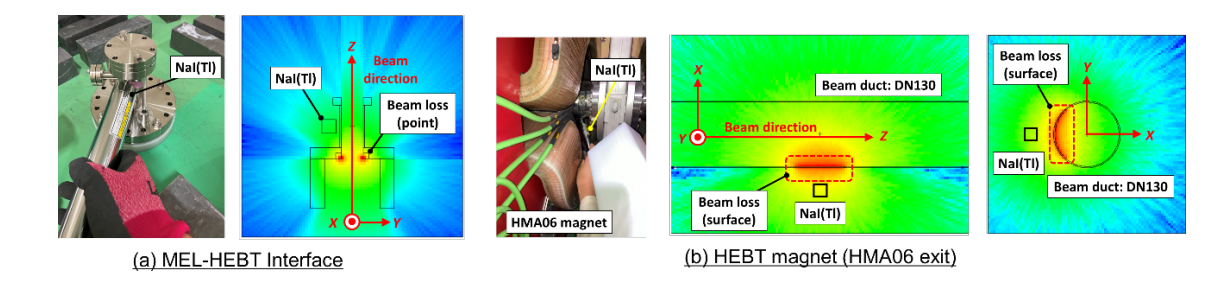


Fig. 3 Dose rate measurements on the beam duct surface at the MEL-HEBT interface and the HEBT magnet (HMA06 exit) using a NaI(Tl) survey meter.

To estimate the deuteron energy associated with beam loss, in-situ gamma spectroscopy was performed using a portable HPGe detector (AMTEK, Inc., GEM20P4-70) placed near the beam duct surface. After beam operation, in-situ HPGe measurements were conducted at the MEL-HEBT interface and the HMA06 exit without radiation shielding. These measurements revealed distinct gamma peaks corresponding to radionuclides produced via deuteron-induced nuclear reactions and secondary neutron interactions with the beamline. The activities of relatively short-lived radionuclides, such as Co-55 ($t_{1/2} = 18$ h), Cu-61 ($t_{1/2} = 3.3$ h), and Tc-96 ($t_{1/2} = 4.3$ d), were compared before and after beam operation. These nuclides are produced exclusively by deuteron interactions with stainless steel. Since their production cross sections depend on deuteron energy as shown in Fig. 4 based on the TENDL-2017 nuclear data library [6], their relative yields serve as energy-dependent indicators for estimating the deuteron energy associated with beam loss.

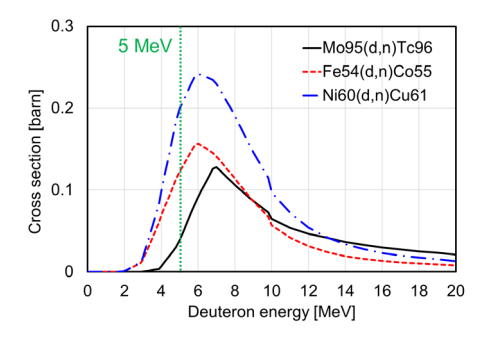


Fig. 4 Cross sections of nuclear reactions leading to the production of Co-55, Cu-61, and Tc-96 as a function of deuteron energy, based on the TENDL-2017 nuclear data library.

In addition to NaI(Tl) survey meter and HPGe measurements, to achieve more accurate beam loss estimation, activation foil measurements were conducted to detect secondary neutrons generated through interactions between lost deuterons and the beam duct. Foils were placed on the beam duct surface at the MEL-HEBT interface and the HMA06 exit. Table 1 summarizes the foil materials, dimensions, associated nuclear reactions, neutron energy thresholds for each reaction, and the half-lives of the resulting daughter nuclides.

TABLE 1. Activation foils used for quantitative beam loss measurement

Foil	Dimension	Reaction	Threshold [MeV]	Half-life
Aluminium	10 x 10 x t1 mm	Al-27(n,α)Na-24	4.9	15.0 h
Nickel	φ15 x t1 mm	Ni-58(n,p)Co-58	1.9	71.6 d
Indium	10 x 10 x t1 mm	In-115(n,n')In-115m	0.5	4.5 h
Gold	10 x 10 x t0.05 mm	A., 107(n a) A., 109	O (Evanneia)	2.7 d
(bare and w/ Cd cover)	(Cd cover: t0.5 mm)	Au-197(n,γ)Au-198	0 (Exoergic)	2./ Q

Because reaction thresholds vary among the foils, neutron energy information can be inferred by analysing their activation levels. After one day of beam operation, gamma rays emitted from each foil were measured using an HPGe detector with lead shielding. Bare gold foils were used to detect thermal neutrons, while cadmium-covered

foils filtered out slow neutrons below 0.5 eV [5]. Measurement durations were typically 1 hour for Al, In, and Au foils, and 10 hours for Ni foils. The activity of each foil, A [Bq], was calculated using Eq. (1) below [5]:

$$A = \frac{C\lambda}{\{1 - \exp(-\lambda t_{\rm m})\}\varepsilon_{\rm f}I_{\rm y}}$$
 Eq. (1)

where C is the net count, λ is the decay constant [s⁻¹], $t_{\rm m}$ is the measurement time [s], $\varepsilon_{\rm f}$ is the HPGe detector efficiency, and I_{γ} is the decay intensity. Since the beam was frequently turned on and off, as shown in Fig. 2, the reaction rate R [atoms/s] was calculated by dividing the activity A by the correction factor B defined below:

$$B = e^{-\lambda(t-t_5)} \left\{ 1 + e^{-\lambda(t_5-t_4)} \left\{ e^{-\lambda(t_4-t_3)} \left\{ 1 + e^{-\lambda(t_3-t_2)} \left[e^{-\lambda(t_2-t_1)} \left(1 - e^{-\lambda t_1} \right) - 1 \right] \right\} - 1 \right\} \right\}$$
 Eq. (2)

where the beam is turned on at t_1 , and turned off at t_2 , on again at t_3 , and so forth. To evaluate beam loss, experimentally derived reaction rates were compared with those calculated using MCNP, based on the simplified geometries shown in Fig. 3. The latest prototype JENDL-5 deuteron sublibrary for Fe(d,xn) reactions was employed in combination with the International Reactor Dosimetry File (IRDF-2002) to model individual reaction channels with enhanced accuracy.

3. RESULTS AND DISCUSSIONS

Fig. 5 shows the results of NaI(Tl) survey meter measurements in both horizontal (X) and vertical (Y) directions, conducted prior to beam operations from June 17 to 19, 2024. Relatively high dose rates were observed at the MEL magnets (LMA02 and LMA03 entrances), the MEL-HEBT interface, and the HEBT magnet (HMA06 exit). These findings suggest that high-energy deuterons were lost at these locations, as activation of the beam duct requires energies exceeding approximately 1 MeV, as indicated by the nuclear reactions shown in Fig. 4. The beam trajectories in horizontal and vertical directions are shown at the bottom of Fig. 5, calculated using beam dynamics simulations. A comparison between the measurements and the simulations reveals elevated dose rates at the following locations:

- Regions where the beam expands transversely,
- The MEL-HEBT interface, where the beam duct narrows (from DN100 to DN40),
- The HMA06 exit, where halo particles are predicted to be generated in -X direction according to simulations.

Table 2 compares measured dose rates taken in the negative Y direction at the MEL-HEBT interface from June 17 to 19 with calculated values. Measurement uncertainties were estimated based on the $\pm 15\%$ accuracy of the NaI(Tl) survey meter. In the previous study [6], the deuteron energy of core particles in the LIPAc was measured to be as 5.0-5.1 MeV using the TOF technique. When the deuteron energy lost at this location is assumed to be 5 MeV, the dose rate increase due to the beam operation on June 18 (i.e. Difference: (2) minus (1) in Table 2) showed good agreement between the measured and calculated values, assuming deuteron loss of 10 μ A. When the same beam loss is assumed at the HMA06 exit, the dose rate increase matched the calculated value at a deuteron energy of 4 MeV. This may indicate that beam loss and/or deuteron energy at the HMA06 exit is lower than at the MEL-HEBT interface.

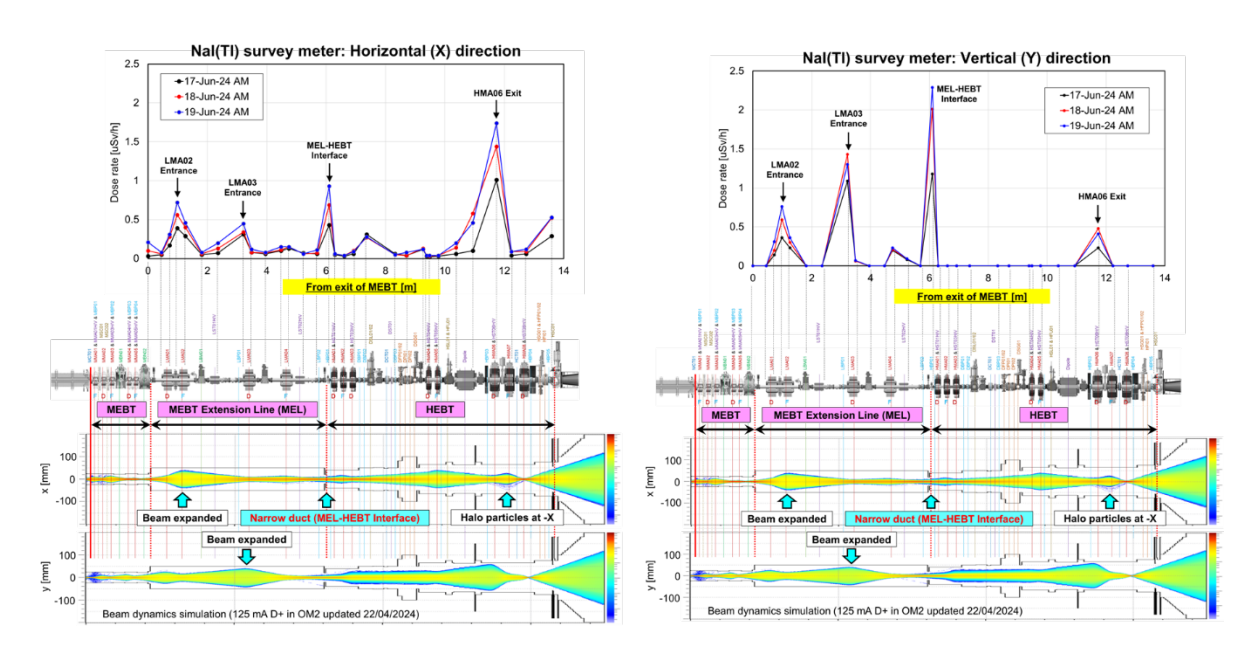


Fig. 5 Dose rates measured by a NaI(Tl) survey meter on the beam duct surface along the LIPAc beamline in the horizontal (X) and vertical (Y) directions. The contour plot at the bottom shows the results of beam dynamics simulations.

TABLE 2. Comparison of dose rate at the MEL-HEBT interface: NaI(Tl) measurements vs. calculations assuming a $10 \mu A$ deuteron loss in the negative Y direction

No.	Measurement - Date	Dose rate [μSv/h]			
		Measurement -	Calculation		
			4 MeV	5 MeV	6 MeV
(0)	June 16 AM	1.18	1.18 (= Measurement)	1.18	1.18
(1)	June 17 AM	2.01	1.24	1.39	1.64
Diffe	erence: $(1) - (0)$	0.83 ± 0.35	0.06	0.21	0.46
(2)	June 18 AM	2.29	1.32	1.67	2.29
Diffe	erence: (2) – (1)	0.28 ± 0.46	0.08	0.28	0.65

TABLE 3. Comparison of dose rate at the HMA06 exit: NaI(Tl) measurements vs. calculations assuming a 10 μ A deuteron loss in the negative *X* direction

No.	Measurement - Date	Dose rate [µSv/h]			
		Measurement	Calculation		
			4 MeV	5 MeV	6 MeV
(0)	June 16 AM	1.01	1.01 (= Measurement)	1.01	1.01
(1)	June 17 AM	1.44	1.28	1.89	2.85
Diffe	erence: (1) – (0)	0.43 ± 0.26	0.27	0.88	1.84
(2)	June 18 AM	1.74	1.66	3.11	5.43
Diffe	erence: (2) – (1)	0.30 ± 0.34	0.38	1.22	2.58

HPGe spectroscopy was conducted to investigate radionuclides generated by core particles lost at the MEL-HEBT interface and by halo particles at the HMA06 exit following the beam operation on June 10, 2024 (See Fig. 2). The dose rate increase at the HMA06 exit, measured by the NaI(Tl) survey meter, was $3.86\pm0.94~\mu Sv/h$, which corresponds to a beam loss approximately ten times greater than those shown in Table 3 (i.e. Differences: (1) minus (0), (2) minus (1)). As shown in Fig. 4, this study focused on deuteron-induced radionuclides generated via the nuclear reactions Mo-95(d,n)Tc-96, Fe-54(d,n)Co-55, and Ni-60(d,n)Cu-61. The Tc-96 peak was below the detection limit ($<3\sigma$) at the HMA06 exit, whereas it was clearly detected at the MEL-HEBT interface. The specific activity of Tc-96 corresponding to the detection limit was estimated to be 63 Bq/kg based on the HPGe spectrum.

Using this value, the deuteron energy of halo particles lost at the HMA06 exit was estimated to be below 3.5 MeV, based on FISPACT-II calculations and NaI(Tl) survey results.

Fig. 6 compares the measured and calculated production ratios of Co-55/Tc-96 at the MEL-HEBT interface and Co-55/Cu-61 at the HMA06 exit, obtained using the portable HPGe detector following the June 10 beam operation. From the production ratios of Tc-96, Co-55, and Cu-61, the deuteron energy of core particles at the MEL-HEBT interface was estimated to be 5.8 MeV (+1.3/-0.5). This value differed from the 5.0 – 5.1 MeV reported in Ref. [6], likely due to uncertainties in the cross-section data in TENDL-2017. Nevertheless, the estimated energy of 4.9 MeV (+1.0/-0.7) for halo particles at the HMA06 exit, obtained from Fig. 6(b), shows a tendency toward lower energy compared to core particles. These findings provide valuable insight into spatial differences in beam loss energy and associated mechanisms, demonstrating the effectiveness of the HPGe measurements in evaluating lost deuteron energy.

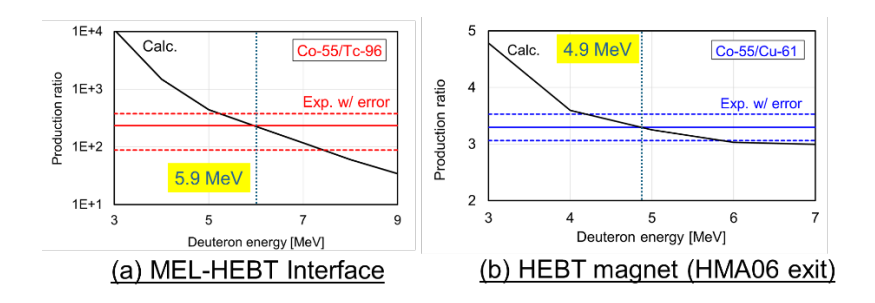


Fig. 6 Comparison between measured and calculated production ratios of Co-55/Tc-96 at the MEL-HEBT interface and Co-55/Cu-61at the HMA06 exit using the HPGe detector following beam operation on June 10, 2024.

Table 4 summarizes activation foil measurements conducted at the MEL-HEBT interface and the HMA06 exit following irradiation during the June 18 beam operation. The absence of activation in the Al foil at both locations indicates that 5 MeV deuterons were not lost at currents exceeding 200 μ A at the MEL-HEBT interface, based on MCNP calculations and the detection limit (< 1.6×10² atoms/s). In contrast, activation of Ni and In foils suggests that high-energy secondary neutrons were generated through deuteron interactions with the beamline. For the Au foil, the measured reaction rates exceeded the calculated values, likely due to contributions from low-energy neutrons produced at multiple locations. The reaction rates of Ni and In foils, which are sensitive to high-energy neutrons, were higher at the MEL-HEBT interface than at the HMA06 exit. These results are consistent with the Tc-96 detection observed in the HPGe measurements. This table also presents calculated reaction rates assuming deuteron energies of 5 MeV and 3.5 MeV for core and halo particles, respectively, based on Ref. [6] and HPGe data. Using these assumptions, beam losses were estimated to be 20 and 100 μ A by matching the calculated reaction rates of Ni and In foils with the measured data. These findings suggest that significant halo particle losses occur at the HMA06 exit, despite the relatively low deuteron energy. Such elevated halo losses may affect not only beamline activation but also other operational aspects, such as increased vacuum pressure.

TABLE 4. Comparison of reaction rate at the MEL-HEBT interface and the HMA06 exit based on activation foil measurements and MCNP calculations for the June 18 beam operation

	Reaction rate [atoms/s]				
	MEL-HEBT interface		HMA06 exit		
Foil	Measurement	Calculation	Measurement	Calculation	
		5 MeV		3.5 MeV	
		20 μΑ		100 μΑ	
Al	N.D. ($< 1.6 \times 10^2$)	1.2×10 ¹	N.D. ($< 1.3 \times 10^2$)	2.3×10^{0}	
Ni	$1.2\pm0.2\times10^{4}$	1.1×10 ⁴	$8.2\pm1.2\times10^{3}$	7.7×10^{3}	
In	$4.2\pm0.1\times10^{3}$	4.6×10^{3}	$3.0\pm0.1\times10^{3}$	3.2×10^{3}	
Au (bare)	$7.8\pm1.3\times10^{2}$	1.5×10 ²	$3.1\pm0.2\times10^{3}$	8.5×10^{1}	
Au w/ Cd	$7.1\pm1.3\times10^{2}$	_	$2.6\pm0.2\times10^{3}$	_	

The estimated beam loss of 5 MeV and 20 μ A for core particles at the MEL-HEBT was consistent with the NaI(Tl) measurements, within the error margins shown in Table 2. In contrast, the halo particle loss of 3.5 MeV and 100 μ A at the HMA06 exit resulted in a discrepancy by a factor of three compared to the NaI(Tl) measurements. This discrepancy may be attributed to differences between the simulation assumptions and actual experimental conditions, such as the temporal uniformity of beam loss and photon source definitions used in MCNP.

4. CONCLUSION

In this study, beam loss characteristics were quantitatively evaluated using a combination of NaI(Tl) survey meter measurements, in-situ HPGe gamma spectroscopy, and activation foil analysis conducted in the LIPAc deuteron accelerator. Core particles lost at the MEL-HEBT interface exhibited higher deuteron energy than halo particles lost at the HEBT magnet (HMA06 exit). However, the experimental results indicated that significantly larger quantities of halo particles were lost compared to core particles. The first quantitative demonstration of beam losses at the LIPAc provides a critical benchmark for future beam loss diagnostics and operational optimization. The observed spatial differences in beam loss and associated deuteron energies highlight the effectiveness of employing multiple radiation diagnostics. Activation and structural damage to beam pipes are expected to become more severe during the upcoming 9 MeV beam campaign in Phase-C/D. As precise evaluation of beam loss and its energy will become increasingly important, dedicated beam operations will be essential for these radiation measurements.

ACKNOWLEDGEMENTS

The authors are grateful to Dr. S. Nakayama in JAEA for providing the latest prototype JENDL-5 deuteron sublibrary for iron.

REFERENCES

- [1] DZITKO, H. et al., "Overview of Broader Approach activities", Fusion Engineering and Design 201 (2024) 114259.
- [2] AKAGI, T. et al., "Accomplishment of high duty cycle beam commissioning of Liner IFMIF Prototype Accelerator (LIPAc) at 5 MeV, 125 mA D⁺", TEC/4-5, paper presented at Synopsis in 30th IAEA Fusion Energy Conference (FEC2025), Chengdu, 2025.
- [3] RISING, M. E. et al., "MCNP® Code Version 6.3.0 Release Notes. Los Alamos National Laboratory Tech. Rep.," LA-UR-22-33103 Rev. 1, Los Alamos National Laboratory (2023).
- [4] SUBLET, J.-CH. et al., "FISPACT-II: An Advanced Simulation System for Activation, Transmutation and Material Modelling", Nuclear Data Sheets 139 (2017) 77–137.
- [5] KNOLL, G., Radiation Detection and Measurement, Third Edition, John Wiley & Sons, Inc., New York (2000).
- [6] HIROSAWA, K. et al., "Measurements of momentum halo due to the reduced RFQ voltage during the LIPAc beam commissioning", Journal of Instrumentation 19 (2024) T05002.
- [7] KONING, A. et al., "TENDL: Complete Nuclear Data Library for Innovative Nuclear Science and Technology", Nuclear Data Sheets, **155** (2019) 1–55.